OCEANOGRAPHY

Microzooplankton grazing on the coccolithophore *Emiliania huxleyi* and its role in the global calcium carbonate cycle

Chloe L. Dean[1,2]*, Elizabeth L. Harvey[3], Matthew D. Johnson[4], Adam V. Subhas[2]

Identifying mechanisms driving the substantial dissolution of biogenic $CaCO_3$ (60 to 80%) in surface and mesopelagic waters of the global ocean is critical for constraining the surface ocean's alkalinity and inorganic carbon budgets. We examine microzooplankton grazing on coccolithophores, photosynthetic calcifying algae responsible for a majority of open-ocean $CaCO_3$ production, as a mechanism driving shallow dissolution. We show that microzooplankton grazing dissolves 92 ± 7% of ingested coccolith calcite, which may explain 50 to 100% of the observed $CaCO_3$ dissolution in supersaturated surface waters. Microzooplankton grazing on coccolithophores is thus a substantial, previously unrecognized biological mechanism affecting the ballasting of organic carbon to deeper waters, the ecology and fitness of microzooplankton themselves due to buffering of food vacuole pH, and ultimately the continued ability of the surface ocean to take up atmospheric carbon dioxide.

INTRODUCTION

The marine calcium carbonate ($CaCO_3$) cycle is a crucial component of the global carbon cycle and ocean carbonate chemistry. It involves the production, export, and dissolution of $CaCO_3$, all of which can affect the ocean's ability to uptake atmospheric CO_2 (*1*). However, uncertainties persist in global production and dissolution rates, preventing an accurate quantification of the magnitude of its contribution to the global carbon cycle (*2*, *3*). One especially paradoxical aspect is the widespread evidence for shallow dissolution of $CaCO_3$ in the upper 1000 m of the ocean water column, which is supersaturated with respect to calcium carbonate and should thermodynamically favor precipitation over dissolution (*1*, *2*, *4*, *5*). Despite the growing consensus around the necessity of shallow dissolution to explain ocean alkalinity distributions, the processes driving shallow dissolution remain unclear (*6*). A role for microenvironments, such as those that form in sinking particles or the acidic guts of zooplankton, has been speculated upon for decades. Since the idea was first put forth by Milliman (*1*), biologically mediated dissolution of biogenic calcite has emerged as a mechanism with promising potential to account for much of the observed $CaCO_3$ dissolution in shallow oceanic regions (*1*, *7*–*9*). However, the importance of this mechanism globally remains unconstrained.

The biogenic calcite produced by coccolithophores represents a prime candidate as a source for biologically mediated dissolution, as these organisms can be responsible for 50 to 90% of pelagic $CaCO_3$ production (*10*) and also serve as foundational primary producers in many marine ecosystems (*11*). In addition, individual coccolithophores sink very slowly out of the surface ocean unless they are aggregated through biological processes, such as grazing and subsequent fecal pellet packaging (*12*, *13*) or transparent exopolymer particle production mediated by stress and/or viral lysis (*14*, *15*). Previous studies have demonstrated that mesozooplankton (size range, 200 to 2000 μm) grazing on coccolithophores can result in up to 73% of ingested calcite dissolving during gut passage (*7*–*9*). Microzooplankton (MZP) may also play a role. These single-cell, heterotrophic protists (size range, 20 to 200 μm) are the primary consumers of photosynthetic nanophytoplankton, such as coccolithophores, in nearly all ocean provinces (*16*, *17*). MZP consume five times more primary production than mesozooplankton and are responsible for ingesting up to 60% of coccolithophore calcite production (*16*, *18*). However, because of the small size of waste "minipellets" produced from MZP grazing, their direct contributions to the vertical flux of carbon are thought to be limited (*19*, *20*). Considering MZP's role as the dominant consumer of marine phytoplankton, we investigated the impact of MZP grazing on the cosmopolitan coccolithophore *Emiliania huxleyi* (*E. hux*) on $CaCO_3$ recycling in the surface ocean (*3*).

Bulk measurements to quantify the ingestion and digestion of coccolith calcite by MZP are complicated by the submicromolar amount of carbon transfer associated with these microscale predators and prey. We cultured *E. hux* (CCMP374) in growth media containing ^{13}C-labeled dissolved inorganic carbon (DIC) and conducted grazing experiments with two model MZP, *Oxyrrhis marina* (*O. mar*) and *Gyrodinium dominans* (*G. dom*). We subsequently quantified inorganic carbon transfer at the nanomolar level via measurements of ^{13}C tracer in the particulate and dissolved phases of the experimental system. Grazing experiments were conducted at a set predator-to-prey ratio (data S1), along with seawater-, predator-, uncalcified (naked) prey–, and calcified prey–only controls (see the Supplementary Materials for additional method details and schematic). We confirmed our geochemical carbon tracking results via microscopy using a semiquantitative pH-sensitive fluorescent probe. We then contextualized our lab-derived estimates of dissolution using global calcium carbonate production, export, and dissolution rates to reconcile disparities between observed trends of production and export.

[1]MIT-WHOI Joint Program in Oceanography/Applied Ocean Science and Engineering, Cambridge and Woods Hole, MA 02543, USA. [2]Marine Chemistry and Geochemistry Department, Woods Hole Oceanographic Institution, Woods Hole, MA 02543, USA. [3]Department of Biological Sciences, University of New Hampshire, Durham, NH 03824, USA. [4]Biology Department, Woods Hole Oceanographic Institution, Woods Hole, MA 02543, USA.
*Corresponding author. Email: chloe.dean@whoi.edu

RESULTS

Substantial calcite dissolution during MZP grazing

Across all experiments, we observed rapid ingestion of coccolithophores by both MZP, coupled with the dissolution of 92 ± 7% of ingested calcite over a 4-hour digestion period (Fig. 1B and data S1). Over the grazing period, both *O. mar* and *G. dom* populations demonstrated similar ranges in particulate inorganic carbon (PIC) ingestion (0.44 ± 0.2; 0.34 ± 0.1 μmol of PIC, respectively; Fig. 1A). *O. mar*, a coastal dinoflagellate, displayed an average 94% (±2%) dissolution of ingested coccolith calcite, while *G. dom*, which is representative of open-ocean dinoflagellates, showed an average 87% (±11%) dissolution (Fig. 1B). Bulk seawater undersaturation–driven dissolution rates of coccolithophore calcite in seawater are on the order of fractions of a percent per day and can only support supersaturated dissolution through the production of metabolic acids in confined microenvironments (*5*). Comparatively, the MZP-mediated dissolution rates reported here (equivalent to 480%/day) are some of the fastest calcite dissolution rates ever measured in seawater and approach the diffusion limit (*21*, *22*).

To account for the mass transfer of PI^{13}C into the dissolved phase, we analyzed DI^{13}C at the beginning and end of the grazing experiments (Fig. 1C). Because of complications associated with filtration and gas exchange, the DI^{13}C provides a qualitative metric for the release of total labeled carbon from the particulate to the dissolved phase. The addition of the "naked" *E. hux* grazing treatment allowed us to constrain the DI^{13}C associated with MZP respiration of organic matter alone, as the naked phenotype of the CCMP374 strain does not calcify. Calcified *E. hux* is characterized by a molar ratio of PIC and particulate organic carbon (POC; PIC:POC, also referred to as the "rain ratio") of ~1 (*23*). The average molar enrichment observed in calcified grazing treatments was more than double that of the enrichment observed in naked grazing treatments (1.97 nmol in calcified versus 0.43 nmol in naked), lending additional confidence that our ^{13}C-labeling approach allowed us to disentangle the isotopic enrichment from digestion of organic and inorganic materials.

We used the pH-dependent LysoSensor probe to visualize pH dynamics semiquantitatively during the progression of digestion for both calcified and noncalcified prey. Microscopy demonstrates active LysoSensor fluorescence within the MZP, colocalized with chlorophyll fluorescence from the prey (Fig. 2, A to D). The LysoSensor pK_a [DND-167, pK_a = 5 (where K_a is the acid dissociation constant)] indicates that these digestive vacuoles are highly acidic (pH < 5), well below both ambient seawater pH and the critical pH for promoting rapid calcite dissolution (*24*).

Using the microscopy images, we calculate a corrected total cell fluorescence (CTCF; Eq. 5 and data S1C) and compare fluorescence intensity, a proxy for vacuole pH, between uncalcified and calcified prey. We find a much lower CTCF (higher pH) in the calcified prey vacuoles and a higher CTCF (lower pH) in vacuoles filled with noncalcified prey [$t(10) = -4.6$, $P = 0.0005$]. The difference in relative pH between these two prey types demonstrates a potential buffering effect that increases pH during calcified prey digestion, through the production of alkalinity from calcite dissolution (Fig. 2E). This buffering effect has been demonstrated within mesozooplankton grazing experiments using *Acartia tonsa* copepods and the coccolithophore *Pleurochrysis carterae* (*9*) and has also been hypothesized to occur during MZP digestion of coccoliths (*25*).

Our CTCF data support the hypothesis that coccolith dissolution leads to the buffering of MZP food vacuoles, but the consequences of a less acidic vacuole remain to be fully elucidated, especially its

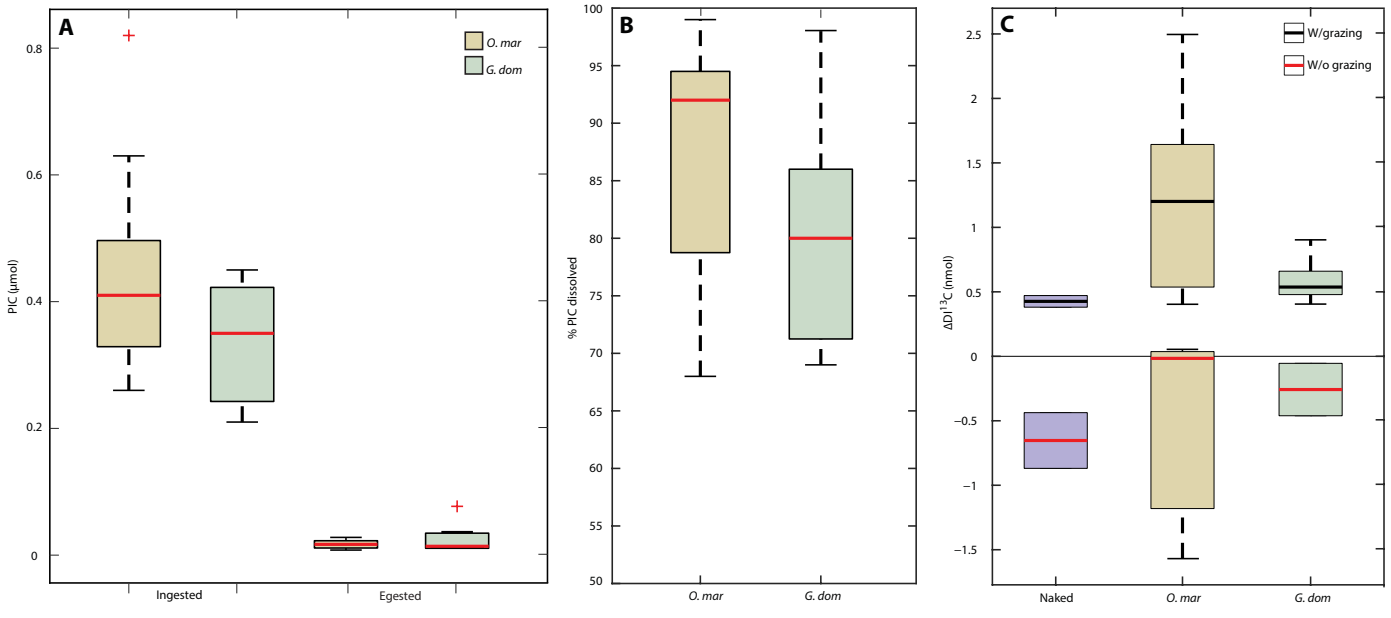

Fig. 1. MZP digestion promotes dissolution of coccolithophore PIC. (**A**) PIC (micromoles) ingested and egested (PIC that remained after the digestion period) for each MZP. (**B**) % PIC dissolved based on the difference between PIC ingested and egested. (**C**) Summary plot of the nanomolar change in DI^{13}C for all grazing experiment treatments, including uncalcified naked controls (purple boxes), prey only ("w/o grazing"; red median line), and grazing treatments ("w/ grazing"; black median line). Zero line is drawn on (C) to indicate no change in DI^{13}C, where any points above the zero line signify molar enrichment of ^{13}C and points below the zero line indicate molar depletion of ^{13}C. All calcified and naked prey treatments where grazing occurred fall above the zero line, indicating release of ^{13}C from the digestion of labeled biomaterials. All control treatments without grazing fall at or below the zero line.

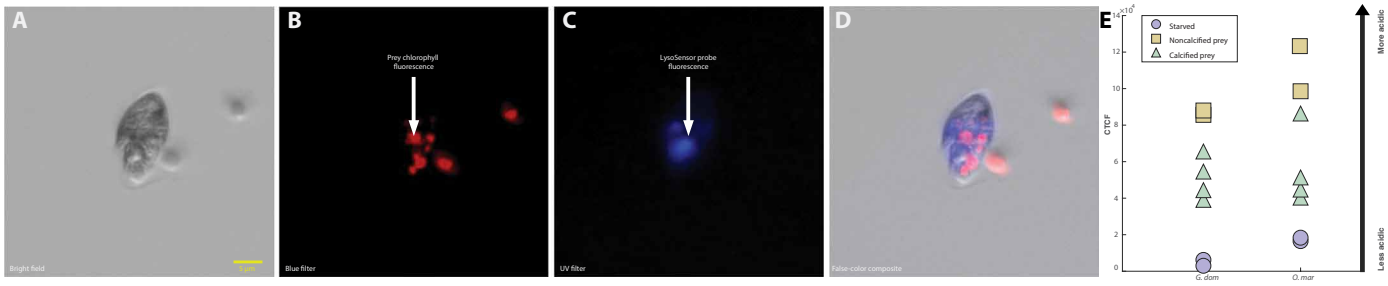

Fig. 2. LysoSensor tracks MZP vacuole pH evolution during digestion of calcified and noncalcified prey. (**A** to **D**) Image series for *O. mar* food vacuoles 3 hours after ingesting calcified *E. hux*. (A) Bright-field image showing engulfed prey and free prey. Scale bar, 5 μm. (B) False-color blue light image showing chlorophyll fluorescence of ingested and free prey. (C) False-color ultraviolet (UV) light image showing LysoSensor probe fluorescence within MZP vacuoles containing prey. (D) False-color composite of images (A to C) overlaid to aid in the visualization of colocalized prey and LysoSensor fluorescence. (**E**) Scatterplot of corrected total cell fluorescence (CTCF); purple circles show CTCF for freshly engulfed prey (t = 0 hours), green triangles show ingestion of calcified prey (CCMP374-C) after 3 hours, and tan squares show ingestion of noncalcified prey (CCMP1323) after 3 hours.

relationship to the fitness and digestive efficiency of natural MZP communities. A food vacuole with lower acidity might lead to decreased efficiency in digesting and assimilating prey, potentially providing a mechanism for the diminished fitness and growth observed in MZP grazers when consuming calcified prey versus noncalcified prey (*25*).

DISCUSSION

The global importance of MZP grazing on upper ocean carbon cycling

Most global models and data syntheses suggest high rates of euphotic $CaCO_3$ production, accompanied by rapid shallow dissolution within the euphotic and mesopelagic zones (Table 1 and references therein). The very fast dissolution rates measured here suggest a plausible mechanism for this rapid dissolution that can be integrated into current literature estimates of coccolithophore production rates and MZP grazing rates

$$PIC_{Dissolved} = (P\_[PIC] \times \%_{coccos}) \times \%_{MZP} \times \%_{Diss} \quad (1)$$

where $P\_[PIC]$ is the globally averaged PIC production rate (Gt PIC year^{-1}), $\%_{coccos}$ is the average proportion of global PIC that is produced by coccolithophores, $\%_{MZP}$ is the average proportion of calcite production grazed by MZP, and $\%_{Diss}$ is the mean proportion of coccolith PIC that dissolves during MZP digestion (Fig. 1B). Calculations were performed for the range of literature values reported in Table 1 using the reported mean production rate, a mean 90% proportion of PIC produced by coccolithophores (*10*, *26*), a mean 60% of calcite production grazed by MZP (*18*), and a mean of 92% PIC dissolution due to MZP grazing, as determined in this study (Fig. 1B). For the remainder of this discussion, any reference to "shallow" or "surface" dissolution is constrained to the euphotic zone (~200 m), given that the majority of reported production and export values reference the base of the photic zone (Table 1).

There now exists a wide range in reported values for global calcium carbonate production, with estimates ranging from 0.5 to 3.7 Gt C year^{-e} (Table 1). The continuous upward trend in global calcium carbonate production estimates can be attributed to several factors, including advances in methodologies and technologies that allow for more accurate measurements (*2*, *5*, *27*) and models (*6*, *28*, *29*) of calcium carbonate cycling, as well as an evolving understanding of the diversity and distribution of calcium carbonate producing organisms (*10*, *30*). The growing global production estimates are also reflected in the associated export (0.2 to 1.8 Gt C year^{-1}) and dissolution rates (0.3 to 2.9 Gt C year^{-1}), which serve to reinforce the significance of the shallow calcium carbonate dissolution flux. Despite these variations, our extrapolated laboratory dissolution rates (0.3 to 1.8 Gt C year^{-1}) generally align well with the reported values of in situ dissolution rates, accounting for 50 to 100% of observed shallow dissolution rates. Together, these estimates reinforce our findings that MZP-mediated dissolution is a central driver of the rapid cycling of $CaCO_3$ in the euphotic zone.

Table 1. Summary of global ocean $CaCO_3$ production, export, and extrapolated MZP dissolution rates.

Data source	Production rate (Gt PIC year^{-1})	Export rate (Gt PIC year^{-1})	Export depth (m)	In situ dissolution rate (Gt PIC year^{-1})	Lab-determined MZP dissolution rate (Gt PIC year^{-1})
Milliman (*1*)	0.6	0.2	100	0.4	0.3
Feely *et al.* (*40*)	0.7	0.4	200–1100	0.3	0.4
Berelson *et al.* (*2*)	0.5–1.6	0.4–1.8	~200	1.0	0.3–0.8
Sulpis *et al.* (*28*)	1.6	0.5–0.9	300	0.6–1.2	0.8
Liang *et al.* (*29*)	1.8–2.0	1.0	279	1.0	0.9–1.0
Ziveri *et al.* (*10*)	3.7	0.7	100–200	2.9	1.8

The important role of MZP in the dissolution of upper ocean $CaCO_3$ is further reinforced when compared with other recognized processes involved in the packaging and processing of biogenic calcite (Fig. 3). Foraminifera and pteropods together likely experience minimal shallow dissolution, as they are expected to quickly sink out of the euphotic and mesopelagic due to their large size (*10*, *13*). Fish-produced carbonates are still highly unconstrained in global $CaCO_3$ production estimates, leaving their contribution to the $CaCO_3$ export and shallow dissolution uncertain (*31*, *32*).

Coccolithophores appear to be the dominant producer of open-ocean calcium carbonate (*10*, *30*). When considering the different processes that affect the attenuation of coccolithophore calcite, only 5% of the calcite ingested by MZP is exported from the euphotic zone (Eq. 1, Fig. 1, and Table 1). Similarly, mesozooplankton processing results in the export of 7% of coccolithophore calcite, but their ultimate contribution to shallow dissolution is likely smaller than MZP due to their different trophic role within food webs (*9*, *16*, *17*). All the remaining coccolithophore production (28%) we assume has the potential to aggregate into marine snow particles, which are large enough to sink rapidly out of the euphotic zone. It is worth noting that this remaining 28% includes the viral loss rate, which can also contribute to aggregation and particle formation (*33*) but may also cause coccolith shedding that may or may not become entrained in particles, thus hindering a full accounting of the fate of $CaCO_3$ associated with these processes.

Alongside MZP grazing, particle-driven dissolution of $CaCO_3$ is emerging as another major biological mechanism that controls attenuation of shallow $CaCO_3$. Recent global estimates of dissolution occurring in waters, supersaturated with respect to calcite but undersaturated with respect to aragonite, imply a dissolution of 30% of

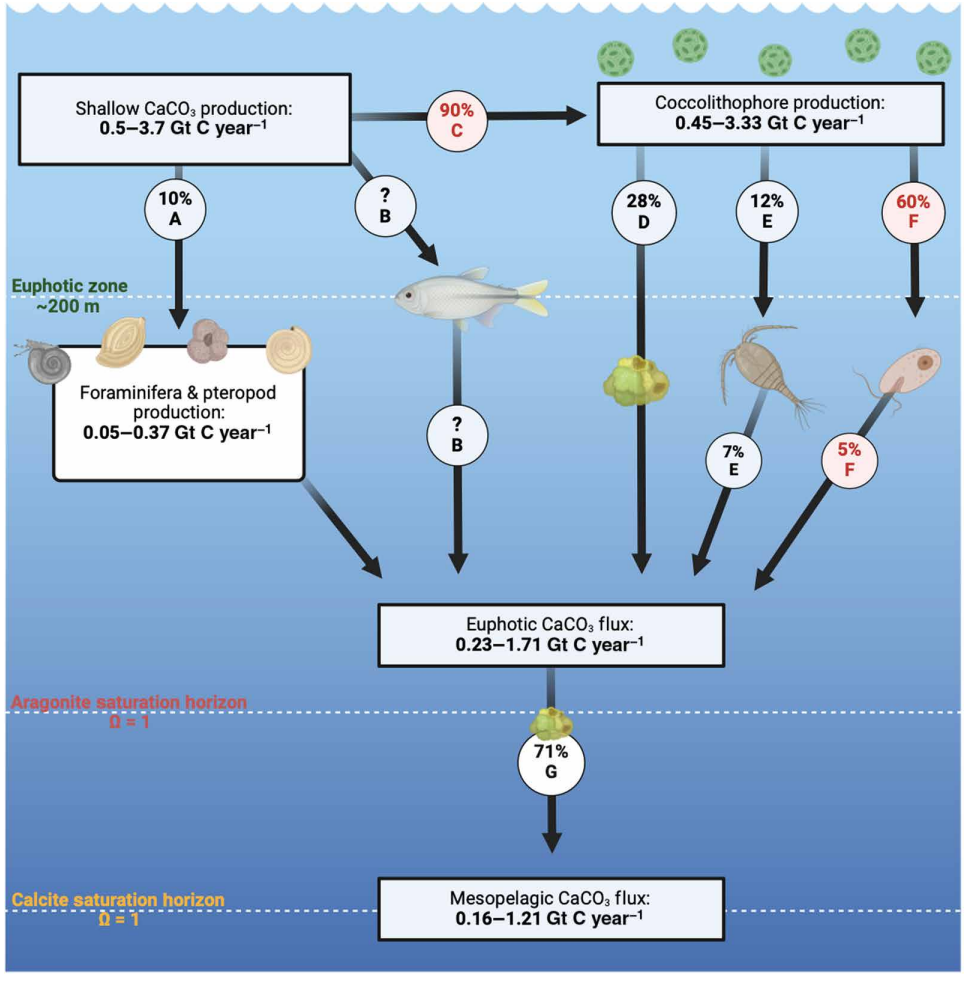

Fig. 3. Fate of biogenic calcium carbonate within the euphotic and mesopelagic ocean. Values in boxes represent the upper and lower bounds for global $CaCO_3$ fluxes. Arrows represent the flux of $CaCO_3$ in percentage, with letters indicating each distinct process. The top dashed line corresponds to the euphotic zone (~200 m), the middle dashed line represents the aragonite saturation horizon, and the bottom dashed line represents the calcite saturation horizon (where all forms of calcium carbonate are undersaturated). Shallow $CaCO_3$ production values are taken from (*2*, *10*). (A) Portion of global $CaCO_3$ production attributed to large calcifying organisms (*10*) which sink directly out of the euphotic zone with minimal shallow dissolution. (B) Portion of global $CaCO_3$ production attributed to fish—now unconstrained (*32*). (C) Portion of global $CaCO_3$ production attributed to coccolithophores (*10*). (D) Portion of coccolithophore production that is not directly grazed and is available for viral lysis and/or aggregation into sinking particles (*16*, *17*). (E) Portion of coccolithophore production grazed by mesozooplankton [12%; (*16*, *17*)] and subsequently dissolved [38%; (*9*)]. (F) Portion of coccolithophore production grazed by MZP [60%; (*16*, *17*)] and subsequently dissolved (92%; this study). (G) Estimated extent of dissolution occurring in "mid-saturated" waters [where waters are supersaturated with respect to calcite but undersaturated with respect to aragonite; 29%; (*6*)].

the euphotic zone flux within mesopelagic waters (*6*). Respiration within sinking particle aggregates may drive the formation of acidic microenvironments that could facilitate further dissolution as they sink from the euphotic zone (*5*). It is also possible for protists, fungi, fish larvae, and micro- and mesozooplankton to feed on and degrade particle aggregates, leading to a now unconstrained dissolution flux within particles that sink below the euphotic zone and deeper in the mesopelagic (*34*, *35*). While particle-driven dissolution represents an unconstrained aspect of the $CaCO_3$ cycle, our study highlights the demonstrative role of MZP ingestion and subsequent dissolution as a fundamental biogeochemical mechanism working to rapidly recycle a substantial portion of $CaCO_3$ within the supersaturated surface ocean.

In the broader context of ocean ecosystems and carbon transport, MZP grazing–mediated dissolution of coccolithophores may reduce the calcite pool available for packaging into heavy, sinking particles. The ballasting of sinking particles by calcium carbonate is proposed to be an important control on the efficiency of the biological carbon pump (BCP), which is how photosynthetically fixed carbon moves from the surface to deep ocean (*11*, *36*). Our results suggest that MZP grazing may reduce the efficiency of the BCP indirectly by reducing the amount of coccolith calcite available for ballasting sinking particles. The modulation of MZP grazing on the ballast effect of coccolith calcite within the context of the BCP remains to be tested and should be explored via direct in situ observations that explicitly measure coccolithophore production, MZP grazing, and particulate export fluxes. Field studies of coccolithophore bloom dynamics with a focus on calcite production, grazing and viral infection mortality rates, associated particle aggregation, and export at various depths would provide a more comprehensive understanding of the dynamic mechanisms that control the calcium carbonate counter pump and, by extension, the ocean's ability to absorb CO_2.

This study identifies MZP grazing as a previously ignored biological mechanism that contributes to the shallow regeneration of alkalinity and, by extension, maintains the buffering capacity of the surface ocean (*6*). The application of ^{13}C labeling in cultures can accurately and reliably quantify micro- and nanoscale processes involving the transformation and movement of carbon. In addition, we have demonstrated a potential time-dependent buffering effect within the food vacuoles of MZP due to the dissolution of ingested calcite materials, which likely affects grazer fitness (*25*) and dynamics of $CaCO_3$ export within natural communities. The extrapolation of our lab results to global production and dissolution rates lends additional confidence in our identification of MZP grazing as an essential mechanism that recycles up to 50% of biogenic calcite production within the surface and mesopelagic ocean. This study highlights the importance of considering biological activity and ecological interactions in the recycling of shallow alkalinity, especially with regard to improving models and predictions of the ocean's ability to absorb atmospheric CO_2.

MATERIALS AND METHODS

General culturing procedures

^{13}C-labeled seawater was prepared using sterile filtered seawater (FSW; 0.2-μm pore size). DIC and total alkalinity (TA) were completely removed via HCl addition and aeration and were then restored to typical surface values (2000 μmol kg^{-1} and 2200 μequiv kg^{-1}, respectively) using ^{13}C-labeled sodium bicarbonate ($NaH^{13}CO_3$) and sodium hydroxide (NaOH). f/2-Si culture medium was prepared according to (*37*) using the ^{13}C-labeled seawater and used to culture *E. hux* (strain CCMP374 from K. Bidle at Rutgers University). Cultures were maintained in exponential growth at 16°C with a light intensity of ~75 μmol photon m^{-2} s^{-1} on a 12/12-hour light/dark cycle. Cultures were allowed to grow under these conditions until their PIC reached a $f^{13}C$ of ~50% before any experiments were performed, with the $f^{13}C$ being the ratio of ^{13}C to total inorganic C ($^{13}C + {}^{12}C$). A minimum value of 50% for $f^{13}C$ was chosen because it allows for substantial enrichment in the $PI^{13}C$ pool, thus providing a useful tracer for the fate of coccolith calcite during grazing.

O. mar and *G. dom* were obtained from the Phyto Lab in the College of Life Sciences and Agriculture at the University of New Hampshire and maintained in the Subhas Lab at the Woods Hole Oceanographic Institution. Cultures were transferred and fed weekly with *Isochrysis galbana* (CCMP1323) to a final concentration of 10,000 cells ml^{-1}. MZP were maintained in an incubator with the same conditions as coccolithophore cultures. Before experiments, MZP were starved in sterile FSW for 5 days to ensure that their vacuoles were empty.

Organism abundance

During experiments, *E. hux* cell density was assessed via triplicate 300-μl aliquots, run on a flow cytometer (Guava, Millipore), with optimized settings determined based on chlorophyll a fluorescence, side scatter (SSC), and forward scatter. To determine MZP abundance, 2-ml aliquots were preserved using 1% Lugol's solution and counted using a Sedgewick-Rafter chamber and a light microscope.

MZP ingestion tests

Before conducting grazing dissolution experiments, ingestion tests were conducted with both MZP to determine the optimal grazing density on non–^{13}C-labeled *E. hux*. Tests were performed using a range of prey-to-predator ratios (50 to 1000) to identify which ratio allowed for the greatest prey ingestion within a 4-hour ingestion period. Prey ingestion was quantified by calculating the change in cell density every hour for 6 hours total. It was determined that a prey-to-predator ratio of ~500 for *O. mar* and ~200 for *G. dom* allowed for maximum ingestion of *E. hux* within a 4-hour period, and all subsequent grazing experiments were performed at that ratio.

Coccolith dissolution experimental protocol

Experimental bottles were prepared at a set prey:predator ratio, along with seawater-, predator-, naked prey–, and calcified prey–only controls. All bottles were sampled for initial measurements ($t = 0$) of organism abundance, PIC, and DIC and placed in an incubator for the 4-hour ingestion period (fig. S1). Total prey ingestion was quantified via flow cytometry by calculating the change in prey abundance over the ingestion period ($t = 4$). MZP were then separated and recovered using a series of FSW rinses through a 5-μm polycarbonate track-etch membrane filter that allowed for uneaten *E. hux* cells to pass through. Recovered MZP were placed in a clean bottle with new FSW and were allowed to digest for another 4-hour period. Following MZP recovery, organism abundances were sampled to verify that the majority of uneaten *E. hux* was removed and that >50% of the initial MZP were recovered. At the end of the 4-hour digestion period ($t = 8$), final samples were collected for organism abundance, PIC, and DIC. Controls were carried through the entire experimental setup.

Corrections for MZP regurgitation of ingested coccolithophores

During the digestion periods, it was observed that some coccolithophore cells were "regurgitated" by the MZP. Regurgitation of cells was first observed on the microscope when confirming that live MZP were recovered following the filtration of uneaten coccolithophores. Within a matter of seconds, an individual MZP was observed to spin rapidly and eject a coccolithophore cell that it had ingested. Haunost *et al.* (*38*) also observed this phenomenon and showed that flow cytometry could be used to quantify the number of partially digested cells that had been regurgitated (they defined this phenomenon as egestion, but here, we use the term "regurgitation"). We inspected the flow cytometry plots and correlated the regurgitated cells to a small population that had a similar SSC value but reduced fluorescence compared to the uneaten *E. hux* (fig. S2). We then corrected our "cells ingested" and subsequent "PIC ingested" calculations by gating and subtracting the regurgitated cells.

PIC ingestion and dissolution calculations

We related the measured cellular PIC quota (picomol PIC per cell) to the number of cells ingested to quantify the amount of PIC ingested during MZP grazing. PIC ingestion was then calculated using the following equation

$$pmol\,PIC_{MZP} = \frac{pmol\,PIC}{cell} \times \left(\frac{cells}{ml}_{i} - \frac{cells}{ml}_{f} \right) \times ml_{exp} \quad (2)$$

where the cell density at the end of the ingestion period $\left(\frac{cells}{ml}_{f}\right)$ is subtracted from the cell density at the start of the grazing experiment $\left(\frac{cells}{ml}_{i}\right)$ and multiplied by the total experimental volume (ml_{exp}) and the cellular PIC quota.

The following equations were used to convert the raw signals from the Picarro into moles dissolved of ^{13}C during MZP grazing. The $f^{13}C$, which is the ratio of $^{13}C/^{tot}C$, was determined using the following equation

$$f^{13} = \left(\frac{DI^{13}C}{DI^{12}C + DI^{13}C} \right) \quad (3)$$

where $DI^{13}C$ is the amount of ^{13}C in the dissolved phase, and $DI^{12}C + DI^{13}C$ is the total DIC. Assuming negligible additions of ^{12}C relative to ^{13}C due to the enrichment of ^{13}C within the coccoliths ($f^{13}C > 50\%$), the change in the isotopic abundance from the start and end of grazing was converted to a change in moles of ^{13}C added to the seawater using the following equation [modified from (*39*)]

$$\Delta DI^{13}C_{(sample,f)-(GRZ,f)} = m_i \times [DIC]_{f/2,i} \times \left(f^{13}_{sample,f} - f^{13}_{GRZ,f} \right) \quad (4)$$

where m_i is the mass of seawater at the start of the grazing experiments, and $[DIC]_{f/2,i}$ is the initial DIC of the f/2-Si media control in micromoles per kilogram. $f^{13}_{sample,f}$ is the fractional abundance measured at the final time point for the treatment, and $f^{13}_{GRZ,f}$ is the fractional abundance measured at the final time point for the grazing-only control. Therefore, $\Delta DI^{13}C_{f-i}$ represents the change in moles of ^{13}C between the start and end of the grazing experiments. Because of unpredictable changes in [DIC] from filtration steps in the experimental method, we chose to use $[DIC]_{f/2,i}$ because it represents the true initial [DIC] without any impacts from biology or other experimental artifacts.

While the PIC data constrain the high end of coccolith dissolution due to confounding effects of regurgitation, or "spitting out" partially digested materials (fig. S2), the $DI^{13}C$ data represent the lower limit of coccolith dissolution due to the potential loss of $^{13}CO_2$ due to outgassing during filtration steps. One-way, single-factor analysis of variance (ANOVA) confirms that the $DI^{13}C$ enrichment in the calcified grazing bottles was significantly different from the enrichment associated with the nongrazing controls ($P < 0.05$; Fig. 1C and data S1). The naked *E. hux* grazing treatment (374-N) allowed us to constrain the $DI^{13}C$ associated with MZP respiration of labeled organic matter and was not statistically different from the enrichment associated with calcified grazing treatments via one-way ANOVA ($P = 0.409$).

Analytical techniques

DIC samples were collected via gravity filtration by passing ~20 ml of seawater through a combusted 0.45-μm glass fiber filter, and PIC samples were taken from the same filters used for DIC collection. PIC samples were dried in an oven at 65°C for a minimum of 4 hours and stored in combusted tin foil inside the fridge until analyzed. All samples were analyzed using a Picarro Cavity Ring-Down Spectroscopy system, allowing simultaneous δ^{13} C and total PIC or DIC determination.

To account for the mass transfer of PIC into the dissolved phase, we also analyzed $DI^{13}C$ at the beginning and end of the grazing experiments (Fig. 1C and fig. S3). Where the PIC data constrain the high end of coccolith dissolution, the $DI^{13}C$ data represent the lower limit of coccolith dissolution due to the potential loss of $^{13}CO_2$ due to outgassing during filtration steps. Other controls were incorporated into the experimental design to correct for various processes that might affect the $PI^{13}C$ and $DI^{13}C$ data. The media-only control served as a constraint on any isotope effects due to filtration and methodological artifacts. The grazer-only control allowed us to account for any effects arising from ambient grazer respiration, which affects [DIC] and appeared to enrich the experiment media in $DI^{12}C$ (e.g., negative values in Fig. 1C). The prey-only control served as a constraint on any background dissolution that occurred on the calcified strains (i.e., from coccolith shedding/disintegration, microbially mediated dissolution, etc).

Vacuole pH determination using LysoSensor probe

Using LysoSensor Blue (DND-167), an acidotropic fluorescent probe, and an epifluorescence microscope equipped with a camera, we evaluated the acidity of food vacuoles during a 3-hour digestion period for both *I. galbana* (noncalcified prey) and *E. hux* (calcified prey). To understand the dynamics of pH evolution as the food vacuole forms and prey is digested, MZP were "pulse-fed" with prey, wherein they were initially starved, fed with prey (10^4 cells/ml), and imaged every ~30 min for 3 hours. Two microliters of the LysoSensor probe was added to 1 ml of the MZP cultures (final probe concentration, 2 μM) and then incubated in darkness for 10 min at room temperature. After incubation, the cultures were anesthetized using 3 μl of $NiSO_4$ per 1 ml of culture to slow MZP movement to obtain clear images. Images were then collected using (i) transmitted light for normal color images, (ii) blue light for chlorophyll fluorescence of prey, and (iii) ultraviolet light for LysoSensor probe fluorescence (Fig. 2B). We then calculated the CTCF associated with the lysosome as follows

$$CTCF = Integrated\ density - (Area\ of\ lysosome \times mean\ background\ fluorescence) \quad (5)$$

See data S1C for raw data and CTCF calculations. See data S2 for all photos collected and used for the CTCF analysis.

Supplementary Materials

The PDF file includes:
Figs. S1 to S3
Legends for data S1 and S2

Other Supplementary Material for this manuscript includes the following:
Data S1 and S2

REFERENCES AND NOTES

1. J. D. Milliman, Production and accumulation of calcium carbonate in the ocean: Budget of a nonsteady state. *Global Biogeochem. Cy.* **7**, 927–957 (1993).
2. W. M. Berelson, W. M. Balch, R. Najjar, R. A. Feely, C. Sabine, K. Lee, Relating estimates of $CaCO_3$ production, export, and dissolution in the water column to measurements of $CaCO_3$ rain into sediment traps and dissolution on the sea floor: A revised global carbonate budget. *Global Biogeochem. Cy.* **21**, doi.org/10.1029/2006GB002803 (2007).
3. M. D. Iglesias-Rodríguez, C. W. Brown, S. C. Doney, J. Kleypas, D. Kolber, Z. Kolber, P. K. Hayes, P. G. Falkowski, Representing key phytoplankton functional groups in ocean carbon cycle models: Coccolithophorids. *Global Biogeochem. Cy.* **16**, 47-1–47-20 (2002).
4. R. Gangstø, M. Gehlen, B. Schneider, L. Bopp, O. Aumont, F. Joos, Modeling the marine aragonite cycle: Changes under rising carbon dioxide and its role in shallow water $CaCO_3$ dissolution. *Biogeosciences* **5**, 1057–1072 (2008).
5. A. V. Subhas, S. Dong, J. D. Naviaux, N. E. Rollins, P. Ziveri, W. Gray, J. W. B. Rae, X. Liu, R. H. Byrne, S. Chen, C. Moore, L. Martell-Bonet, Z. Steiner, G. Antler, H. Hu, A. Lunstrum, Y. Hou, N. Kemnitz, J. Stutsman, S. Pallacks, M. Dugenne, P. Quay, W. M. Berelson, J. F. Adkins, Shallow calcium carbonate cycling in the North Pacific Ocean. *Global Biogeochem. Cy.* **36**, e2022GB007388 (2022).
6. E. Y. Kwon, J. P. Dunne, K. Lee, Biological export production controls upper ocean calcium carbonate dissolution and CO_2 buffer capacity. *Sci. Adv.* **10**, eadl0779 (2024).
7. R. R. Harris, Zooplankton grazing on the coccolithophore *Emiliania huxleyi* and its role in inorganic carbon flux. *Mar. Biol.* **119**, 431–439 (1994).
8. G. Langer, G. Nehrke, S. Jansen, Dissolution of *Calcidiscus leptoporus* coccoliths in copepod guts? A morphological study. *Mar. Ecol. Prog. Ser.* **331**, 139–146 (2007).
9. M. M. White, J. D. Waller, L. C. Lubelczyk, D. T. Drapeau, B. C. Bowler, W. M. Balch, D. M. Fields, Coccolith dissolution within copepod guts affects fecal pellet density and sinking rate. *Sci. Rep.* **8**, 9758 (2018).
10. P. Ziveri, W. R. Gray, G. Anglada-Ortiz, C. Manno, M. Grelaud, A. Incarbona, J. W. B. Rae, A. V. Subhas, S. Pallacks, A. White, J. F. Adkins, W. Berelson, Pelagic calcium carbonate production and shallow dissolution in the North Pacific Ocean. *Nat. Commun.* **14**, 805 (2023).
11. B. Rost, U. Riebesell, "Coccolithophores and the biological pump: Responses to environmental changes" in *Coccolithophores: From Molecular Processes to Global Impact*, H. R. Thierstein, J. R. Young, Eds. (Springer, 2004), pp. 99–125.
12. L. T. Bach, U. Riebesell, S. Sett, S. Febiri, P. Rzepka, K. G. Schulz, An approach for particle sinking velocity measurements in the 3–400 µm size range and considerations on the effect of temperature on sinking rates. *Mar. Biol.* **159**, 1853–1864 (2012).
13. A. V. Subhas, F. J. Pavia, S. Dong, P. J. Lam, Global trends in the distribution of biogenic minerals in the ocean. *J. Geophys. Res. Oceans* **128**, e2022JC019470 (2023).
14. J. I. Nissimov, A. Pagarete, F. Ma, S. Cody, D. D. Dunigan, S. A. Kimmance, M. J. Allen, Coccolithoviruses: A review of cross-kingdom genomic thievery and metabolic thuggery. *Viruses* **9**, 52 (2017).
15. U. Sheyn, S. Rosenwasser, Y. Lehahn, N. Barak-Gavish, R. Rotkopf, K. D. Bidle, I. Koren, D. Schatz, A. Vardi, Expression profiling of host and virus during a coccolithophore bloom provides insights into the role of viral infection in promoting carbon export. *ISME J.* **12**, 704–713 (2018).
16. C. Schmoker, S. Hernández-León, A. Calbet, Microzooplankton grazing in the oceans: Impacts, data variability, knowledge gaps and future directions. *J. Plankton Res.* **35**, 691–706 (2013).
17. D. K. Steinberg, M. R. Landry, Zooplankton and the ocean carbon cycle. *Annu. Rev. Mar. Sci.* **9**, 413–444 (2017).
18. K. M. J. Mayers, A. J. Poulton, C. J. Daniels, S. R. Wells, E. M. S. Woodward, G. A. Tarran, C. E. Widdicombe, D. J. Mayor, A. Atkinson, S. L. C. Giering, Growth and mortality of coccolithophores during spring in a temperate Shelf Sea (Celtic Sea, April 2015). *Prog. Oceanogr.* **177**, 101928 (2019).
19. M. M. Gowing, M. W. Silver, Minipellets: A new and abundant size class of marine fecal pellets. *J. Mar. Res.* **43**, 395–418 (1985).
20. K. Beaumont, G. Nash, A. Davidson, Ultrastructure, morphology and flux of microzooplankton faecal pellets in an east Antarctic fjord. *Mar. Ecol. Prog. Ser.* **245**, 133–148 (2002).
21. A. V. Subhas, J. F. Adkins, N. E. Rollins, J. Naviaux, J. Erez, W. M. Berelson, Catalysis and chemical mechanisms of calcite dissolution in seawater. *Proc. Natl. Acad. Sci. U.S.A.* **114**, 8175–8180 (2017).
22. E. L. Sjöberg, D. T. Rickard, Calcite dissolution kinetics: Surface speciation and the origin of the variable pH dependence. *Chem. Geol.* **42**, 119–136 (1984).
23. K. M. Krumhardt, N. S. Lovenduski, M. D. Iglesias-Rodriguez, J. A. Kleypas, Coccolithophore growth and calcification in a changing ocean. *Prog. Oceanogr.* **159**, 276–295 (2017).
24. J. D. Naviaux, A. V. Subhas, N. E. Rollins, S. Dong, W. M. Berelson, J. F. Adkins, Temperature dependence of calcite dissolution kinetics in seawater. *Geochim. Cosmochim. Acta* **246**, 363–384 (2019).
25. E. L. Harvey, K. D. Bidle, M. D. Johnson, Consequences of strain variability and calcification in *Emiliania huxleyi* on microzooplankton grazing. *J. Plankton Res.* **37**, 1137–1148 (2015).
26. R. Schiebel, Planktic foraminiferal sedimentation and the marine calcite budget. *Global Biogeochem. Cy.* **16**, 3-1–3-21 (2002).
27. G. Neukermans, L. T. Bach, A. Butterley, Q. Sun, H. Claustre, G. R. Fournier, Quantitative and mechanistic understanding of the open ocean carbonate pump - perspectives for remote sensing and autonomous in situ observation. *Earth-Sci. Rev.* **239**, 104359 (2023).
28. O. Sulpis, E. Jeansson, A. Dinauer, S. K. Lauvset, J. J. Middelburg, Calcium carbonate dissolution patterns in the ocean. *Nat. Geosci.* **14**, 423–428 (2021).
29. H. Liang, A. M. Lunstrum, S. Dong, W. M. Berelson, S. G. John, Constraining $CaCO_3$ export and dissolution with an ocean alkalinity inverse model. *Global Biogeochem. Cy.* **37**, e2022GB007535 (2023).
30. N. S. Knecht, F. Benedetti, E. U. Hofmann Elizondo, N. Bednaršek, S. Chaabane, C. De Weerd, K. T. C. A. Peijnenburg, R. Schiebel, M. Vogt, The impact of zooplankton calcifiers on the marine carbon cycle. *Global Biogeochem. Cy.* **37**, e2022GB007685 (2023).
31. R. W. Wilson, F. J. Millero, J. R. Taylor, P. J. Walsh, V. Christensen, S. Jennings, M. Grosell, Contribution of fish to the marine inorganic carbon cycle. *Science* **323**, 359–362 (2009).
32. A. M. Oehlert, J. Garza, S. Nixon, L. Frank, E. J. Folkerts, J. D. Stieglitz, C. Lu, R. M. Heuer, D. D. Benetti, J. del Campo, F. A. Gomez, M. Grosell, Implications of dietary carbon incorporation in fish carbonates for the global carbon cycle. *Sci. Total Environ.* **916**, 169895 (2024).
33. C. P. Laber, J. E. Hunter, F. Carvalho, J. R. Collins, E. J. Hunter, B. M. Schieler, E. Boss, K. More, M. Frada, K. Thamatrakoln, C. M. Brown, L. Haramaty, J. Ossolinksi, H. Fredericks, J. I. Nissimov, R. Vandzura, U. Sheyn, Y. Lehahn, R. J. Chant, A. M. Martins, M. J. L. Coolen, A. Vardi, G. R. DiTullio, B. A. S. Van Mooy, K. D. Bidle, *Coccolithovirus* facilitation of carbon export in the North Atlantic. *Nat. Microbiol.* **3**, 537–547 (2018).
34. J. K. B. Bishop, R. W. Collier, D. R. Kettens, J. M. Edmond, The chemistry, biology, and vertical flux of particulate matter from the upper 1500 m of the Panama Basin. *Deep Sea Res.* **27**, 615–640 (1980).
35. K. Tsukamoto, M. J. Miller, The mysterious feeding ecology of leptocephali: A unique strategy of consuming marine snow materials. *Fish. Sci.* **87**, 11–29 (2021).
36. C. L. De La Rocha, U. Passow, Factors influencing the sinking of POC and the efficiency of the biological carbon pump. *Deep Sea Res. Pt. II: Trop. Stud. Oceanogr.* **54**, 639–658 (2007).
37. R. R. L. Guillard, "Culture of phytoplankton for feeding marine invertebrates" in *Culture of Marine Invertebrate Animals*, W. L. Smith, M. H. Chanley, Eds. (Plenum Press, 1975), pp. 26–60.
38. M. Haunost, U. Riebesell, F. D'Amore, O. Kelting, L. T. Bach, Influence of the calcium carbonate shell of coccolithophores on ingestion and growth of a dinoflagellate predator. *Front. Marine Science.* **8**, 664269 (2021).
39. A. V. Subhas, N. E. Rollins, W. M. Berelson, S. Dong, J. Erez, J. F. Adkins, A novel determination of calcite dissolution kinetics in seawater. *Geochim. Cosmochim. Acta* **170**, 51–68 (2015).
40. R. A. Feely, C. L. Sabine, K. Lee, F. J. Millero, M. F. Lamb, D. Greeley, J. L. Bullister, R. M. Key, T.-H. Peng, A. Kozyr, T. Ono, C. S. Wong, In situ calcium carbonate dissolution in the Pacific Ocean. *Global Biogeochem. Cyc.* **16**, 91-1–91-12 (2002).

Acknowledgments: We thank K. Thamatrokoln, K. Bidle, and L. Haramaty (Rutgers) for providing the calcified and naked phenotypes of *E. hux* (CCMP374), as well as culturing expertise. We thank M. Hayden (WHOI) for helping with preliminary method development and experimental design. We acknowledge and thank the editors and reviewers for helpful comments and feedback. **Funding:** This work was supported by the National Sciences Foundation (GCR 2020878 to A.V.S. and E.L.H.). **Author contributions:** Conceptualization: A.V.S., E.L.H., and C.L.D. Methodology: C.L.D., E.L.H., A.V.S., and M.D.J. Resources: A.V.S., M.D.J., and C.L.D. Investigation: C.L.D. and M.D.J. Data curation: C.L.D. and A.V.S. Visualization: C.L.D. Formal analysis: C.L.D. and A.V.S. Validation: C.L.D. and A.V.S. Funding acquisition: A.V.S. and E.L.H. Project administration: A.V.S. and C.L.D. Supervision: A.V.S., E.L.H., M.D.J., and C.L.D. Writing—original draft: C.L.D. Writing—review and editing: C.L.D., A.V.S., E.L.H., and M.D.J. **Diversity, equity, ethics, and inclusion:** We acknowledge that Woods Hole Oceanographic Institution (WHOI) is located on the unceded ancestral and contemporary land of the

Wôpanâak people. We recognize the perpetuated detrimental effects that systemic government oppressions have had on Indigenous communities as a result of colonization. We are committed to taking action to interrupt the legacies of colonialism and build authentic and mutual relationships with Indigenous communities toward justice. **Competing interests:** The authors declare that they have no competing interests. **Data and materials availability:** The dataset and statistics generated for the current study are available as the Supplementary Materials alongside this manuscript. Experimental data and statistics are included in the Excel workbook "data S1," and all LysoSensor microscopy photos are included in the zip file "data S2." Datasets are also available at www.bco-dmo.org/project/865363.

Submitted 5 July 2024
Accepted 7 October 2024
Published 8 November 2024
10.1126/sciadv.adr5453